Available online at www.sciencedirect.com
SCIENCE DIRECT®
Journal of Solid State Chemistry 179 (2006) 2164–2173
JOURNAL OF SOLID STATE CHEMISTRY
www.elsevier.com/locate/jssc

# Structural and conductivity studies of $CsKSO_4Te(OH)_6$ and $Rb_{1.25}K_{0.75}SO_4Te(OH)_6$ materials

N. Chabchoub[a,*], J. Darriet[b], H. Khemakhem[a]

[a]*Laboratoire de Physique Appliquée, Faculté des Sciences de Sfax, 3018 Sfax, Tunisie*
[b]*Institut de Chimie de la Matière Condensée de Bordeaux, ICMCB-CNRS, 33608 Pessac cedex, France*

Received 9 March 2006; received in revised form 12 April 2006; accepted 16 April 2006
Available online 25 April 2006

**Abstract**

The crystal structures of the title compounds were solved using the single-crystal X-ray diffraction technique. At room temperature $CsKSO_4Te(OH)_6$ was found to crystallize in the monoclinic system with *Pn* space group and lattice parameters: $a = 12.5463(6)$ Å; $b = 6.5765(2)$ Å; $c = 12.6916(7)$ Å; $\beta = 106.53(2)^\circ$; $V = 1003.914(4)$ Å$^3$; $Z = 4$ and $D_{calc.} = 3.29$ g/cm$^3$. The structural refinement has led to a reliability factor of $R_1 = 0.0284$ ($wR_2 = 0.064$) for 7577 independent reflections. $Rb_{1.25}K_{0.75}SO_4Te(OH)_6$ material possesses a monoclinic structure with space group $P2_1/a$ and cell parameters: $a = 11.3411(6)$ Å; $b = 6.5819(2)$ Å; $c = 13.5730(8)$ Å; $\beta = 106.860(10)^\circ$; $V = 969.62(10)$ Å$^3$; $Z = 4$ and $D = 3.16(3)$ g/cm$^3$. The residuals are $R_1 = 0.0297$ and $wR_2 = 0.0776$ for 3336 independent reflections. The main interest of these structures is the presence of two different and independent anionic groups ($TeO_6^{6-}$ and $SO_4^{2-}$) in the same crystal.

Complex impedance measurements ($Z^* = Z' - iZ''$) have been undertaken in the frequency and temperature ranges 20–$10^6$ Hz and 400–600 K, respectively. The dielectric relaxation is studied in the complex modulus formalism $M^*$.
© 2006 Elsevier Inc. All rights reserved.

*Keywords:* Sulfate tellurate; Crystal structure; X-ray diffraction; Modulus formalism

## 1. Introduction

A great deal of attention was paid to the preparation and investigation on compounds having general formula $M_2AO_4Te(OH)_6$ (where $M = K$, Rb, Na, Tl, $NH_4$ and Cs, $A = S$, Se and P). In fact, these hydrogen-bonded systems exhibit many interesting physical properties and successive phase transitions. The presence of protons $H^+$ in $Te(OH)_6$ groups, which are in the origin of the network hydrogen bonds, renders possible ionic conductivity in these materials at high temperature [1–9].

A careful examination of the literature show that a large number of alkali metal sulfate and selenate tellurate are presently known and a systematic survey of their crystallographic data has been investigated [2–4,6,8,9]. Similarly, the atomic arrangements usually exhibit anionic groups $TeO_6^{6-}$ and $AO_4^{2-}$ ($A = S$, Se) organized in number of planes connected by network hydrogen bonds. However, the crystal structure of the title compounds has not yet been investigated. The new mixed solid solution, $Rb_{1.25}K_{0.75}SO_4Te(OH)_6$, and $Rb_2SO_4Te(OH)_6$ are isostructural and crystallize in the monoclinic space group $P2_1/a$ [6] whereas, $CsKSO_4Te(OH)_6$ structure's is different from the structure of the original compounds ($K_2SO_4Te(OH)_6$ and $Cs_2SO_4Te(OH)_6$). Indeed, $Cs_2SO_4Te(OH)_6$ exhibits a trigonal structure with the non-centrosymmetric space group *R*3 [8], whereas the structure of the potassium sulfate tellurate $K_2SO_4Te(OH)_6$ is triclinic $P\bar{1}$ [2].

In previous papers, [10–13] we have shown, using dielectric and Raman studies, that the compounds of general formula $MM'(SO_4)\cdot Te(OH)_6$ with ($M$, $M' = K$, Rb and Cs) are ferroelectric in their low temperature phases and exhibit superionic behavior in their high temperature phases. We have also shown that the transition temperatures depend on the alkali cation. In order to examine the influence of cationic substitution over crystalline symmetry and confirm the presence and the character of the hydrogen bonds in $MM'SO_4Te(OH)_6$, we have studied and discussed, in this paper, the results of the

*Corresponding author. Fax: +216 74 27 44 37.
*E-mail address:* nizar_chabchoub@yahoo.fr (N. Chabchoub).

0022-4596/$ - see front matter © 2006 Elsevier Inc. All rights reserved.
doi:10.1016/j.jssc.2006.04.020

crystal structure of two new mixed compounds $CsKSO_4Te(OH)_6$ and $Rb_{1.25}K_{0.75}SO_4Te(OH)_6$. Also, in the present work, the electrical conduction and dielectric relaxation of $Rb_{1.25}K_{0.75}SO_4Te(OH)_6$ have been studied.

## 2. Experimental details

Single crystals of $CsK(SO_4)\cdot Te(OH)_6$ and $Rb_{1.25}K_{0.75}SO_4Te(OH)_6$ were grown by slow evaporation from a mixed aqueous solution containing stoichiometric ratio of potassium sulfate ($K_2SO_4$), telluric acid ($H_6TeO_6$) and $M_2SO_4$ ($M$ = Cs, Rb). The chemical reaction is

$$xK_2SO_4 + (1-x)M_2SO_4 + H_6TeO_6 \rightarrow M_{2-2x}K_{2x}SO_4\cdot Te(OH)_6.$$

Crystals were grown at room temperature under the atmospheric pressure. Approximately after 10 days crystals were isolated. The formulas of the two materials were determined by structural refinement. The selection of a good single crystal was based upon the size and the sharpness of the diffraction spots. Data collections were performed on a Bruker–Nonius Kappa CCD diffractometer using Mo$K\alpha$ radiation. The frame images were integrated using Eval-14 software [14]. Measured intensities were corrected for Lorentz and polarization effects. A Gaussian-type absorption correction was applied, and the shape was determined with the video microscope of the Kappa CCD. The structures were solved using the JANA 2000 package [15].

Because of the small size of single crystals, we use pellets with 7 mm in diameter and about 1 mm in thickness for the dielectric and electric experiments. Before measurements the samples are first tempered at 150 °C for 12 h under vacuum. This heat treatment is used in order to eliminate, as much as possible, the water content in the pellets pores.

The complex impedance, $Z^*$, measurements are performed using an HP 4284A impedance analyzer for the frequency and temperature ranges between 20 Hz and 1 MHz and 400–600 K, respectively. The two main faces of the pellet are pasted with silver plaster as electrodes.

## 3. Results and discussion

### 3.1. Structural study

#### 3.1.1. Structure of $CsKSO_4Te(OH)_6$

At room temperature $CsKSO_4Te(OH)_6$ is monoclinic. The space group is *Pn*. The unit cell dimensions are $a = 12.5463(6)$ Å; $b = 6.5765(2)$ Å; $c = 12.6916(7)$ Å; $\beta = 106.53(2)^\circ$ and $Z = 4$. Crystal data and experimental conditions of the data collection are gathered in Table 1. The final atomic coordinates and are given in Table 2 whereas the bond lengths and angles, including those for the hydrogen bonds, are listed in Table 3.

Fig. 1 shows a projection on the *ac* plane of $CsKSO_4Te(OH)_6$ structure. As one can see from this figure, the arrangement of $Te(OH)_6$ octahedra and $SO_4$ tetrahedra forms rows parallel to the plan $(\bar{1}10)$. Within these rows, the $Te(OH)_6$ octahedrons and $SO_4$ tetrahedrons are connected by hydrogen bonds. We note that they are other hydrogen bonds linking $Te(OH)_6$ octahedron and $SO_4$ tetrahedron belonging to two different rows. These hydrogen bonds existing between the rows reinforce the structure's cohesion. According to the *b*-axis, the rows constitute layers parallel to the $(\bar{1}01)$. The cohesion of the structure is assured by the atoms of potassium and cesium which are ordered in alternating planes parallel to $(\bar{1}01)$ (Fig. 1).

Table 1
Crystallographic data for $CsK(SO_4)\cdot Te(OH)_6$

| Compound | $CsKSO_4Te(OH)_6$ |
|---|---|
| Formula weight | 497.7 g mol$^{-1}$ |
| Temperature | 293 K |
| Crystal system | Monoclinic |
| Space group | *Pn* |
| Unit cell dimensions | $a = 12.5463(6)$ Å; $b = 6.5765(2)$ Å; $c = 12.6916(7)$ Å; $\beta = 06.53(2)^\circ$ |
| Volume | 1003.914(4) Å$^3$ |
| $Z$ | 4 |
| Density (calculated) | 3.29 g cm$^{-3}$ |
| Radiation/wavelength | 0.71073 Å |
| $F(000)$ | 912 |
| $\theta$ range for data collection | 2.01–40.00° |
| Index ranges | $-22\leqslant h\leqslant 22$; $-11\leqslant k\leqslant 11$; $-22\leqslant l\leqslant 22$ |
| Reflections collected | 42210 |
| Observed reflections | 11,558 with $I>3\sigma(I)$ |
| Independent reflections | 7577 with $I>3\sigma(I)$ |
| GOF | 1.17 |
| Weights | $W^{-1}=\sigma(I)^2+0.0009I^2$ |
| Structure refinement | $F^2$ |
| $R$ (%) | 2.84 |
| w$R$ (%) | 6.4 |
| Extinction coefficient | 0.384(9) |
| Absorption coefficient | 7.192 mm$^{-1}$ |
| Absorption correction | Gaussian |
| $T_{min}/T_{max}$ | 0.281/0.461 |

The Te atom in $CsKSO_4Te(OH)_6$ structure occupies two special positions (Table 2). Therefore, the structure shows two types of octahedra. The distances of Te(1)–O vary from 1.868(7) to 1.912(8) Å and O–Te(1)–O angles between the ranges 86.3(3)–93.0(4)° and 175.3(4)–179.4(3)° (Table 4) while in $Te(2)O_6$ octahedra the distances of Te(2)–O are between 1.890(8) and 1.943(7) Å and the O–Te(2)–O angles between the ranges 86.9(4)–94.2(5)° and 175.2(4)–178.5(3)°. So, we can deduce that these octahedra are slightly deformed knowing that $Te(2)O_6$ octahedra is more distorted than $Te(1)O_6$ octahedra. We note that the values of Te–O distances are close to those observed in the original compounds. Indeed, in $Cs_2SO_4\cdot Te(OH)_6$ material, the Te atom occupies only one general position and the Te–O distances spread from 1.905 to 1.907 Å [8] but they are between 1.914 and 1.928 Å in $K_2SO_4\cdot Te(OH)_6$ [2].

Table 2
Fractional atomic coordinates and equivalent isotropic displacement ($U_{iso}$, for H atoms) for $CsK(SO_4)\cdot Te(OH)_6$

| Atom | Occupancy | $x$ | $y$ | $z$ | $U_{eq}$ (Å$^2$) |
|---|---|---|---|---|---|
| Cs1 | 1 | 0 | 0.52167(15) | 0 | 0.0258(3) |
| Cs2 | 1 | 0.23362(2) | −0.97837(14) | −0.77278(3) | 0.0263(3) |
| K1 | 1 | 0.9855(3) | −0.0353(5) | 0.5161(3) | 0.0304(9) |
| K2 | 1 | −0.7510(3) | −0.5327(5) | −1.2914(3) | 0.0261(8) |
| Te1 | 1 | 0.14091(8) | 0.00572(12) | −0.15061(7) | 0.01421(19) |
| Te2 | 1 | 0.09402(7) | −0.49413(12) | −0.61978(7) | 0.01282(18) |
| S1 | 1 | −0.12935(18) | 0.0003(4) | 0.0922(2) | 0.0137(6) |
| S2 | 1 | 0.3630(2) | −0.4987(4) | −0.8616(2) | 0.0160(6) |
| O1 | 1 | −0.2277(6) | 0.0118(12) | −0.0096(6) | 0.0225(16) |
| O2 | 1 | −0.1231(6) | −0.2042(9) | 0.1389(6) | 0.031(2) |
| O3 | 1 | −0.1425(6) | 0.1497(9) | 0.1759(5) | 0.0174(16) |
| O4 | 1 | −0.0294(7) | 0.0474(13) | 0.0604(7) | 0.036(3) |
| O5 | 1 | 0.4585(7) | −0.4808(12) | −0.7681(7) | 0.031(2) |
| O6 | 1 | 0.3744(7) | −0.3475(12) | −0.9432(6) | 0.033(2) |
| O7 | 1 | 0.2599(5) | −0.4593(12) | −0.8328(6) | 0.0223(19) |
| O8 | 1 | 0.3590(6) | −0.7058(9) | −0.9077(6) | 0.024(2) |
| O9 | 1 | 0.2923(6) | 0.0140(13) | −0.1538(6) | 0.024(2) |
| O10 | 1 | −0.0082(6) | −0.0052(13) | −0.1466(6) | 0.027(2) |
| O11 | 1 | 0.1642(6) | 0.2505(12) | −0.0710(7) | 0.035(2) |
| O12 | 1 | 0.0908(7) | 0.1528(15) | −0.2813(6) | 0.033(2) |
| O13 | 1 | 0.1196(7) | −0.2309(14) | −0.2410(7) | 0.029(2) |
| O14 | 1 | 0.1817(6) | −0.1503(14) | −0.0202(6) | 0.0344(19) |
| O15 | 1 | −0.0554(6) | −0.4846(12) | −0.6116(6) | 0.023(2) |
| O16 | 1 | 0.2436(6) | −0.5079(11) | −0.6313(6) | 0.0202(17) |
| O17 | 1 | 0.0488(7) | −0.6307(15) | −0.7576(6) | 0.038(2) |
| O18 | 1 | 0.1100(7) | −0.7363(14) | −0.5364(8) | 0.037(3) |
| O19 | 1 | 0.1435(6) | −0.3365(12) | −0.4850(6) | 0.0236(17) |
| O20 | 1 | 0.0697(7) | −0.2376(12) | −0.6980(6) | 0.034(2) |
| H9 | 1 | 0.311(5) | −0.067(7) | −0.211(3) | 0.040(5) |
| H10 | 1 | −0.025(5) | 0.043(9) | −0.080(3) | 0.040(5) |
| H11 | 1 | 0.233(3) | 0.265(10) | −0.011(3) | 0.040(5) |
| H12 | 1 | 0.046(4) | 0.277(6) | −0.279(6) | 0.040(5) |
| H13 | 1 | 0.067(4) | −0.324(8) | −0.225(4) | 0.040(5) |
| H14 | 1 | 0.247(4) | −0.236(12) | −0.018(7) | 0.040(5) |
| H15 | 1 | −0.074(6) | −0.503(6) | −0.542(3) | 0.040(5) |
| H16 | 1 | 0.250(6) | −0.512(8) | −0.707(3) | 0.040(5) |
| H17 | 1 | −0.020(4) | −0.712(11) | −0.769(7) | 0.040(5) |
| H18 | 1 | 0.184(3) | −0.798(9) | −0.510(5) | 0.040(5) |
| H19 | 1 | 0.210(3) | −0.262(8) | −0.490(6) | 0.040(5) |
| H20 | 1 | −0.0103(19) | −0.221(10) | −0.728(4) | 0.040(5) |

Table 3
Main interatomic distances (Å) and bond angles (deg) in the $CsK(SO_4)\cdot Te(OH)_6$ material

| Distance (Å) | | Angles (deg) | |
|---|---|---|---|
| (a) *Cesium environment* | | | |
| Cs1–O2$^{i}$ | 3.208(8) | Cs2–O1$^{iv}$ | 3.243(8) |
| Cs1–O4 | 3.258(9) | Cs2–O7$^{v}$ | 3.292(8) |
| Cs1–O5$^{ii}$ | 3.303(9) | Cs2–O8 | 3.024(9) |
| Cs1–O7$^{iii}$ | 3.349(6) | Cs2–O10$^{iv}$ | 3.181(7) |
| Cs1–O11 | 3.126(8) | Cs2–O14$^{vi}$ | 3.225(8) |
| Cs1–O14$^{i}$ | 3.201(9 | Cs2–O17 | 3.301(10 |
| Cs1–O16$^{ii}$ | 3.175(7) | Cs2–O20$^{v}$ | 3.186(8) |
| Cs1–O17$^{iii}$ | 3.048(9) | | |
| (b) *Potassium environment* | | | |
| K1–O6$^{vii}$ | 2.993(9) | K2–O2$^{xii}$ | 2.676(8) |
| K1–O8$^{viii}$ | 2.805(9) | K2–O3$^{xiii}$ | 2.948(7) |
| K1–O9$^{ix}$ | 2.751(7) | K2–O12$^{xiv}$ | 2.895(10) |
| K1–O12$^{x}$ | 2.820(8) | K2–O13$^{xv}$ | 2.757(8) |
| K1–O18$^{xi}$ | 2.71(1) | K2–O15$^{xvi}$ | 2.838(7) |
| K1–O19$^{x}$ | 2.688(9) | K2–O19$^{xv}$ | 2.752(10) |

Table 3 (*continued*)

| Distance (Å) | | Angles (deg) | |
|---|---|---|---|
| (c) *Sulfate groups* | | | |
| S1–O1 | 1.513(7) | O1–S1–O2 | 109.3(4) |
| S1–O2 | 1.463(7) | O1–S1–O3 | 110.3(4) |
| S1–O3 | 1.490(7) | O1–S1–O4 | 108.1(5) |
| S1–O4 | 1.456(10) | O2–S1–O3 | 108.8(4) |
| | | O2–S1–O4 | 110.8(4) |
| | | O3–S1–O4 | 109.7(4) |
| | | O5–S2–O6 | 107.6(5) |
| S2–O5 | 1.431(8) | O5–S2–O7 | 111.7(5) |
| S2–O6 | 1.474(8) | O5–S2–O8 | 109.2(4) |
| S2–O7 | 1.464(8) | O6–S2–O7 | 108.9(5) |
| S2–O8 | 1.478(7) | O6–S2–O8 | 110.2(4) |
| | | O7–S2–O8 | 109.3(4) |
| (d) *Tellurate groups* | | | |
| Te1–O9 | 1.912(8) | O9–Te1–O10 | 179.4(3) |
| Te1–O10 | 1.887(8) | O9–Te1–O11 | 89.1(3) |
| Te1–O11 | 1.882(7) | O9–Te1–O12 | 93.0(4) |
| Te1–O12 | 1.868(7) | O9–Te1–O13 | 88.9(3) |
| Te1–O13 | 1.907(7) | O9–Te1–O14 | 90.6(3) |
| Te1–O14 | 1.889(7) | O10–Te1–O11 | 91.2(3) |
| | | O10–Te1–O12 | 87.6(4) |
| | | O10–Te1–O13 | 90.9(3) |
| | | O10–Te1–O14 | 88.8(3) |
| | | O11–Te1–O12 | 89.6(3) |
| | | O11–Te1–O13 | 175.3(4) |
| | | O11–Te1–O14 | 91.9(3) |
| | | O12–Te1–O13 | 86.3(3) |
| | | O12–Te1–O14 | 176.1(3) |
| | | O13–Te1–O14 | 92.4(3) |
| Te2–O15 | 1.908(8) | O15–Te2–O16 | 178.5(3) |
| Te2–O16 | 1.926(8) | O15–Te2–O17 | 91.4(3) |
| Te2–O17 | 1.905(9) | O15–Te2–O18 | 86.9(4) |
| Te2–O18 | 1.890(8) | O15–Te2–O19 | 90.5(3) |
| Te2–O19 | 1.943(7) | O15–Te2–O20 | 89.2(3) |
| Te2–O20 | 1.935(7) | O16–Te2–O17 | 87.1(3) |
| | | O16–Te2–O18 | 93.0(4) |
| | | O16–Te2–O19 | 91.0(3) |
| | | O16–Te2–O20 | 91.0(3) |
| | | O17–Te2–O18 | 94.2(5) |
| | | O17–Te2–O19 | 175.6(4) |
| | | O17–Te2–O20 | 88.7(4) |
| | | O18–Te2–O19 | 89.9(3) |
| | | O18–Te2–O20 | 175.2(4) |
| | | O19–Te2–O20 | 87.3(3) |

| (e) *Hydrogen bonds* | | | | |
|---|---|---|---|---|
| O–H···O | O–H | H···O | O···O | O–H···O |
| O9–H9···O3$^{xix}$ | 0.98(5) | 1.78(5) | 2.740(11) | 165(5) |
| O10–H10···O4 | 0.98(5) | 1.80(4) | 2.736(12) | 159(5) |
| O11–H11···O8$^{iii}$ | 0.98(3) | 1.75(3) | 2.733(9) | 177(5) |
| O12–H12···O5$^{ii}$ | 1.00(5) | 1.76(5) | 2.756(11) | 174(6) |
| O13–H13···O5$^{xvii}$ | 0.96(5) | 1.84(5) | 2.719(11) | 151(4) |
| O14–H14···O6$^{xviii}$ | 1.00(6) | 1.76(5) | 2.671(10) | 149(7) |
| O15–H15···O6$^{xvii}$ | 0.98(5) | 1.85(6) | 2.763(12) | 153(3) |
| O16–H16···O7 | 0.99(5) | 1.67(5) | 2.643(11) | 166(5) |
| O17–H17···O3$^{vi}$ | 0.98(6) | 1.76(5) | 2.720(12) | 166(8) |
| O18–H18···O1$^{iv}$ | 0.98(4) | 1.79(5) | 2.676(11) | 148(5) |
| O19–H19···O1$^{xix}$ | 0.99(5) | 1.87(5) | 2.750(10) | 147(4) |
| O20–H20···O2$^{xx}$ | 0.97(3) | 1.87(4) | 2.709(10) | 142(4) |

*Symmetry codes*: (i) $x$, $1+y$, $z$; (ii) $-0.5+x$, $-y$, $0.5+z$; (iii) $x$, $1+y$, $1+z$; (iv) $0.5+x$, $-1-y$, $-0.5+z$; (v) $x$, $-1+y$, $z$; (vi) $x$, $-1+y$, $-1+z$; (vii) $0.5+x$, $-y$, $1.5+z$; (viii) $0.5+x$, $-1-y$, $1.5+z$; (ix) $0.5+x$, $-y$, $0.5+z$; (x) $1+x$, $y$, $1+z$; (xi) $1+x$, $1+y$, $1+z$; (xii) $-0.5+x$, $-1-y$, $-1.5+z$; (xiii) $-0.5+x$, $-y$, $-1.5+z$; (xiv) $-1+x$, $-1+y$, $-1+z$; (xv) $-1+x$, $y$, $-1+z$; (xvi) $-0.5+x$, $-1-y$, $-0.5+z$; (xvii) $-0.5+x$, $-1-y$, $0.5+z$; (xviii) $x$, $y$, $1+z$; (xix) $0.5+x$, $-y$, $-0.5+z$; (xx) $x$, $y$, $-1+z$; (xxi) $0.5+x$, $-1-y$, $0.5+z$; (xxii) $-0.5+x$, $-y$, $-0.5+z$.

In contrast with the cesium sulfate tellurate [8] and the cesium ammonium sulfate tellurate [16], the structure of $CsKSO_4Te(OH)_6$ presents two types of tetrahedra of $SO_4$.

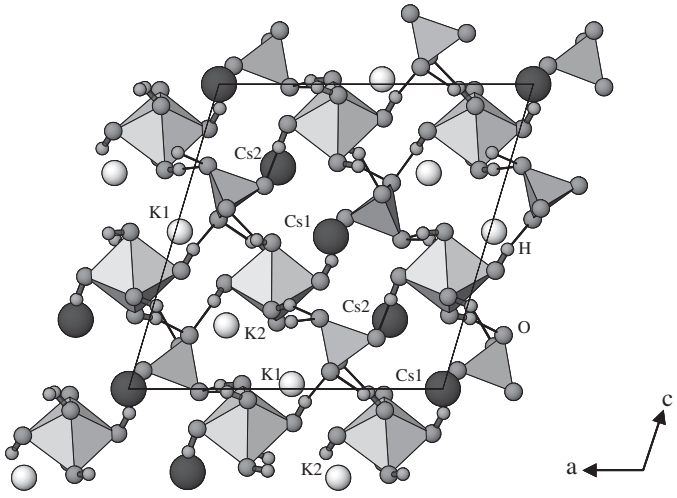


Fig. 1. Projection of $CsK(SO_4)\cdot Te(OH)_6$ crystal structure on the *ac* plane.

Table 4
Crystallographic data for $Rb_{1.25}K_{0.75}SO_4Te(OH)_6$

| Compound | $Rb_{1.25}K_{0.75}SO_4Te(OH)_6$ |
|---|---|
| Formula weight | 462.30 g mol$^{-1}$ |
| Temperature | 293 K |
| Crystal system | Monoclinic |
| Space group | $P2_1/a$ |
| Unit cell dimensions | $a = 11.3411(6)$ Å; $b = 6.5819(2)$ Å; $c = 13.5730(8)$ Å; $\beta = 106.860(10)^\circ$ |
| Volume | 969.62 (10) Å$^3$ |
| $Z$ | 4 |
| Density (calculated) | 3.1657 (3) g cm$^{-3}$ |
| Radiation/wavelength | 0.71069 Å |
| $F$ (000) | 859 |
| $\theta$ range for data collection | 3.14–39.99° |
| Index ranges | $-20\leqslant h\leqslant 20; -11\leqslant k\leqslant 11; -24\leqslant l\leqslant 24$ |
| Reflections collected | 44483 |
| Observed reflections | $5969 I > 3\sigma(I)$ |
| Independent reflections with | $3336 I > 3\sigma(I)$ |
| GOF | 1.41 |
| Weights | $W^{-1} = \sigma(I)^2 + 0.0009I^2$ |
| $R$ (%) | 2.97 |
| w$R$ (%) | 7.76 |
| Structure refinement | $F^2$ |
| Extinction coefficient | 0.098(9) |
| Absorption coefficient | 8.734 |
| Absorption correction | Gaussian |
| $T_{min}/T_{max}$ | 0.148/0.389 |

In the first tetrahedra $S(1)O_4$, the length of the S–O bond varies between 1.456(10) and 1.513(7) Å and angles O–S(1)–O vary from 108.1(5) to 110.8(4)°, whereas in $S(2)O_4$ tetrahedra the minimum and the maximum S–O distances are 1.431(8) and 1.478(7) Å (Table 3), and angles O–S(2)–O range from 107.6(5) to 111.7(5)°. Then, $\Delta$(S–O) and $\Delta$(O–S–O) are 0.057 Å and 2.7° in S(1) and 0.047 Å and 4.1° in S(2) so the shape of $S(2)O_4$ tetrahedra is more regular than $S(1)O_4$. But both are distorted.

In comparison with the cesium sulfate tellurate compound, where one cation $Cs^+$ is coordinated by ten oxygen atoms (six are of $TeO_6$ origin and four belong to the sulfate tetrahedra) and the other is coordinated by nine oxygen atoms [8], the two cesium cations in $CsKSO_4Te(OH)_6$ structure are coordinated by only eight oxygen atoms (Cs(1)) and seven oxygen atoms (Cs(2)). The Cs(1)–O distances are included between 3.047(8) and 3.349(6) Å and the Cs(2)–O distances values vary from 3.026(9) and 3.300(11) Å.

The potassium atoms are distributed on two sites. Both K(1) and K(2) are surrounded by six oxygen atoms as in the case of $K_2SO_4Te(OH)_6$ structure [2] and different to $K_2SO_4Te(OH)_6$ [5], where the cations are coordinated by nine oxygen atoms. In $CsKSO_4Te(OH)_6$ structure, every cation $K^+$ is coordinated by two oxygen atoms belonging to $SO_4$ tetrahedra, two to $Te(1)O_6$ octahedron and two from $Te(2)O_6$ octahedron. The distances K–O vary from 2.688(9) to 2.990(8) Å for the first potassium atom and they are between 2.676(9) and 2.948(7) Å for the second one whereas in $K_2SO_4Te(OH)_6$ structure, the K–O distances vary from 2.713 to 2.987 Å [2].

The $CsKSO_4Te(OH)_6$ structure, is stable thanks to network of hydrogen bonds, assured by hydrogen atoms belonging to $Te(OH)_6$ octahedra. The hydrogen positions have been determined by difference Fourier map.

In the mixed compound, all the oxygen atoms belonging to $SO_4$ groups contribute to the establishment of the hydrogen bonds differently from the original compound $Cs_2SO_4Te(OH)_6$ where only two hydrogen bonds O–H···O are detected [8]. Thus, all hydrogen atoms belonging to $Te(OH)_6$ octahedrons participate in the formation of hydrogen bonding. In sulfate group, two oxygen atoms (O(2)/O(4) for $S(1)O_4$ and O(7)/O(8) for S(2)O) are tied to one hydrogen atom, but each other oxygen atoms (O(1)/O(3) for $S(1)O_4$ and O(5)/O(6) for $S(2)O_4$) are tied to two hydrogen atoms (see Table 3). The O···O distances range between 2.643(11) and 2.763(12) Å, which confirm that they are two types of hydrogen bonds: strong bonds when the O···O are smaller than 2.7 Å and weak in the other case [17]. The O···H distances varying from 1.67(5) to 1.87(5) Å with O–H···O angles ranging from 142(4) to 177(5)° whereas in $Cs_2SO_4Te(OH)_6$, the O···O distances are 2.395(7) and 2.499(2) Å and the O–H···O angles are 119.4(4)–117.24(8)°. This difference explains the effect of cationic substitution over hydrogen bond then over the physical properties. Indeed, all these values of O···H and O–H···O distances can favor the appearance of superprotonic phase transition at high temperature. This deduction was confirmed by dielectric and conductivity measurement [13].

### 3.1.2. Structure of $Rb_{1.25}K_{0.75}SO_4Te(OH)_6$

$Rb_{1.25}K_{0.75}SO_4Te(OH)_6$ crystallizes with a monoclinic symmetry, space group $P2_1/a$ and cell parameters: $a = 11.3411(6)$ Å; $b = 6.5819(2)$ Å; $c = 13.5730(8)$ Å and $\beta = 106.860(10)^\circ$. The residuals are $R_1 = 0.0297$ and

w$R_2 = 0.0776$ for 3336 independent reflections ($I > 3\sigma(I)$). The crystallographic data and some details of the structure refinement are summarized in Table 4. The final atomic positions are reported in Table 5. The main interatomic distances and angles, including those for the hydrogen bonds, are listed in Table 6.

A projection of the $Rb_{1.25}K_{0.75}SO_4Te(OH)_6$ crystal structure on the *ac* plane is depicted in Fig. 2. This figure shows a structural arrangement that is different from the original compounds $K_2SO_4 \cdot Te(OH)_6$ and $Rb_2SO_4 \cdot Te(OH)_6$ [2,6] but similar to $CsKSO_4 \cdot Te(OH)_6$.

The structure can be regarded as being built of planes of mixed polyhedra: $TeO_6$ octahedra and $SO_4$ tetrahedra, parallel to the plan $(\bar{1}01)$, and the $Rb^+/K^+$ cations assure the cohesion between them. In a direction parallel to $(\bar{1}01)$, the $TeO_6$ octahedra and $SO_4$ tetrahedra form infinite rows which are connected by hydrogen bonds in order to reinforce the structure's cohesion. Within these rows the two types of anion ($TeO_6^{6-}$ and $SO_4^{2-}$) are also connected by hydrogen bonds. According to the *b*-axis, the cations form planes parallel to the $(\bar{1}01)$ plan.

Like in the original compounds structure, $K_2SO_4 Te(OH)_6$ and $Rb_2SO_4 \cdot Te(OH)_6$ [2,6], Te atoms are distributed on two sites. Each Te atom is coordinated by six oxygen atoms which form a slightly deformed octahedron around it. Indeed, the $Te(1)O_6$ octahedron has two Te(1)–O distances of 1.901(2) Å, two bond lengths of 1.903(3) Å and two others of 1.917(7) Å. These distances are comparable to those obtained in the original compounds. In reality, in $Rb_2SO_4Te(OH)_6$ material, the Te–O distances spread from 1.903(4) to 1.921(4) Å [6] and they are between 1.914 and 1.928 Å in $K_2SO_4 \cdot Te(OH)_6$ [2]. The second type of $Te(2)O_6$ octahedra have two Te(2)–O distances of 1.908(2), two bond lengths of 1.909(2) Å and two others of 1.910(9) Å (Table 6). In consequence, the $Te(1)O_6$ octahedron is more deformed than the second one. The O–Te(1)–O angles between the ranges 87.18(9)–92.82(9)° and 179.99(9)–180.00(7)° whereas in $Te(2)O_6$ octahedron they spread from 89.17(9)–90.83(9) to 179.99(9)–180.00(0)°. In comparison to the $CsKSO_4$-$Te(OH)_6$ and $Rb_{1.12}(NH_4)_{0.88}SO_4Te(OH)_6$ materials [18], where the structures present two types of tetrahedra of $SO_4$, the sulfur atom in $Rb_{1.25}K_{0.75}SO_4Te(OH)_6$, occupies only one general position as in $Rb_2SO_4Te(OH)_6$ and $Rb_2(SO_4)_{0.5}(SeO_4)_{0.5}Te(OH)_6$ structures [6,19]. The tetrahedral coordination of S atom is built up by four oxygen atoms with S–O distances varying from 1.461(3) to 1.475(2) Å, i.e., in the range of lengths that occur most frequently for sulfate tellurate compounds. The O–S–O angles values in the $SO_4$ groups are between 107.44(14) and 110.79(14)° indicating that the $SO_4$ tetrahedron is slightly distorted.

In $Rb_{1.25}K_{0.75}SO_4Te(OH)_6$ structure, $Rb^+$ and $K^+$ are statistically disordered on one atomic position (Table 4). Similarly to the rubidium sulfate tellurate structure, the Rb/K atoms are distributed on two sites and they are nine coordinated. On the direction parallel to $(\bar{1}01)$ (Fig. 2) one can notice the *M*(1)–*M*(1)–*M*(2)–*M*(2)–*M*(1)–*M*(1) succession (*M* = Rb or K):

- Environment of Rb(1)/K(1): Three oxygen atoms belonging to $SO_4$ tetrahedron, three to $Te(1)O_6$ octahedron, two to another $Te(1)O_6$ and only one to $Te(2)O_6$ octahedron. The Rb(1)/K(1)–O distances are included between 2.980(2) and 3.206(2) Å.

Table 5
Fractional atomic coordinates and equivalent isotropic displacement ($U_{iso}$, for H atoms) for $Rb_{1.25}K_{0.75}SO_4Te(OH)_6$

| Atom | Occupancy | *x* | *y* | *z* | $U_{eq}$ |
|---|---|---|---|---|---|
| Rb1/K1 | 0.753(3)/0.247(3) | 0.09810(4) | 0.00267(4) | 0.35702(3) | 0.02714(12) |
| Rb2/K2 | 0.506(3)/0.494(3) | 0.34447(4) | 0.01649(5) | 0.14261(3) | 0.02284(13) |
| Te1 | 1 | 0 | 0.5 | 0.5 | 0.01305(6) |
| Te2 | 1 | 0.5 | 0.5 | 0 | 0.01276(6) |
| S | 1 | 0.23266(6) | 0.50901(8) | 0.24754(4) | 0.01427(16) |
| O1 | 1 | 0.6097(2) | 0.0055(3) | 0.17196(17) | 0.0277(6) |
| O2 | 1 | 0.23730(18) | 0.3764(3) | 0.33616(13) | 0.0227(6) |
| O3 | 1 | 0.2545(2) | 0.7203(3) | 0.28096(16) | 0.0321(7) |
| O4 | 1 | 0.3281(2) | 0.4395(4) | 0.20255(17) | 0.0358(8) |
| O5 | 1 | 0.06590(19) | 0.6097(3) | 0.63572(13) | 0.0234(6) |
| O6 | 1 | 0.39841(19) | 0.2638(3) | −0.01843(14) | 0.0225(6) |
| O7 | 1 | 0.58466(18) | 0.4126(3) | 0.13641(13) | 0.0208(6) |
| O8 | 1 | 0.1462(2) | 0.5837(4) | 0.46954(17) | 0.0358(8) |
| O9 | 1 | 0.38240(18) | 0.6412(3) | 0.05049(15) | 0.0232(6) |
| O10 | 1 | 0.0662(2) | 0.2376(3) | 0.54115(16) | 0.0344(8) |
| H5 | 1 | 0.124(4) | 0.732(6) | 0.635(3) | 0.057(6) |
| H6 | 1 | 0.394(4) | 0.199(5) | −0.0836(19) | 0.057(6) |
| H7 | 1 | 0.593(4) | 0.274(3) | 0.120(3) | 0.057(6) |
| H8 | 1 | 0.173(6) | 0.501(4) | 0.413(4) | 0.057(6) |
| H9 | 1 | 0.335(4) | 0.564(5) | 0.084(3) | 0.057(6) |
| H10 | 1 | 0.119(3) | 0.251(6) | 0.6110(17) | 0.057(6) |

Table 6
Main interatomic distances (Å) and bond angles (deg) in the $Rb_{1.25}K_{0.75}SO_4Te(OH)_6$ material

| Distance (Å) | | Angles (deg) | | | |
|---|---|---|---|---|---|
| (a) *Rubidium and potassium environment* | | | | | |
| *M*1 = Rb1/K1 and *M*2 = Rb2/K2 | | | | | |
| *M*1–O2 | 2.980(2) | *M*2–O1 | | | 2.918(2) |
| *M*1–O3$^{iii}$ | 2.954(3) | *M*2–O3$^{iii}$ | | | 3.079(3) |
| *M*1–O4$^{iv}$ | 3.192(2) | *M*2–O4 | | | 2.922(3) |
| *M*1–O5$^{i}$ | 3.176(2) | *M*2–O5$^{v}$ | | | 2.948(10) |
| *M*1–O7$^{iv}$ | 3.006(2) | *M*2–O6 | | | 2.929(5) |
| *M*1–O8$^{iii}$ | 3.122(3) | *M*2–O6$^{vii}$ | | | 3.241(2) |
| *M*1–O8$^{v}$ | 3.206(2) | *M*2–O7$^{iv}$ | | | 2.960(2) |
| *M*1–O10 | 3.048(3) | *M*2–O9$^{iii}$ | | | 2.857(2) |
| *M*1–O10$^{vi}$ | 3.063(3) | *M*2–O9$^{vii}$ | | | 3.202(20) |
| (b) *Sulfate groups* | | | | | |
| S–O1$^{iv}$ | 1.475(2) | O1$^{iv}$–S–O2 | 109.38(11) | O2–S–O3 | 110.32(12) |
| S–O2 | 1.475(2) | O1$^{iv}$–S–O3 | 108.56(12) | O2–S–O4 | 107.44(14) |
| S–O3 | 1.462(2) | O1$^{iv}$–S–O4 | 110.79(14) | O3–S–O4 | 110.37(14) |
| S–O4 | 1.461(3) | | | | |
| (c) *Tellurate groups* | | | | | |
| Te1–O5 | 1.917(7) | O5–Te1–O5$^{i}$ | 180.00(7) | O6–Te2–O6$^{ii}$ | 179.99(9) |
| Te1–O5$^{i}$ | 1.917(7) | O5–Te1–O8 | 88.76(9) | O6–Te2–O7 | 89.79(8) |
| Te1–O8 | 1.903(3) | O5–Te1–O8$^{i}$ | 91.24(9) | O6–Te2–O7$^{ii}$ | 90.21(8) |
| Te1–O8$^{i}$ | 1.903(3) | O5–Te1–O10 | 92.82(9) | O6–Te2–O9 | 89.17(9) |
| Te1–O10 | 1.901(2) | O5–Te1–O10$^{i}$ | 87.18(9) | O6–Te2–O9$^{ii}$ | 90.83(9) |
| Te1–O10$^{i}$ | 1.901(2) | O5$^{i}$–Te1–O5 | 180.00(7) | O6$^{ii}$–Te2–O6 | 179.99(9) |
| Te2–O6 | 1.908(2) | O5$^{i}$–Te1–O8 | 91.24(9) | O6$^{ii}$–Te2–O7 | 90.21(8) |
| Te2–O6$^{ii}$ | 1.908(2) | O5$^{i}$–Te1–O8$^{i}$ | 88.76(9) | O6$^{ii}$–Te2–O7$^{ii}$ | 89.79(8) |
| Te2–O7 | 1.910(9) | O5$^{i}$–Te1–O10 | 87.18(9) | O6$^{ii}$–Te2–O9 | 90.83(9) |
| Te2–O7$^{ii}$ | 1.910(9) | O5$^{i}$–Te1–O10$^{i}$ | 92.82(9) | O6$^{ii}$–Te2–O9$^{ii}$ | 89.17(9) |
| Te2–O9 | 1.909(2) | O8–Te1–O8$^{i}$ | 180.0(1) | O7–Te2–O7$^{ii}$ | 180.00(8) |
| Te2–O9$^{ii}$ | 1.909(2) | O8–Te1–O10 | 91.84(10) | O7–Te2–O9 | 90.33(8) |
| | | O8–Te1–O10$^{i}$ | 88.16(10) | O7–Te2–O9$^{ii}$ | 89.67(8) |
| | | O8$^{i}$–Te1–O8 | 180.0(1) | O7$^{ii}$–Te2–O7 | 180.00(8) |
| | | O8$^{i}$–Te1–O10 | 88.16(10) | O7$^{ii}$–Te2–O9 | 89.67(8) |
| | | O8$^{i}$–Te1–O10$^{i}$ | 91.84(10) | O7$^{ii}$–Te2–O9$^{ii}$ | 90.33(8) |
| | | O10–Te1–O10$^{i}$ | 179.99(9) | O9–Te2–O9$^{ii}$ | 179.99(9) |
| | | O10$^{i}$–Te1–O10 | 179.99(9) | O9$^{ii}$–Te2–O9 | 179.99(9) |
| (d) *Hydrogen bonds* | | | | | |
| O–H···O | O–H | H···O | O···O | O–H···O | |
| O5–H5···O2$^{ix}$ | 1.04(4) | 1.78(4) | 2.778(3) | 159(3) | |
| O6–H6···O1$^{xi}$ | 0.98(3) | 1.79(3) | 2.718(3) | 157(3) | |
| O7–H7···O1 | 0.95(2) | 1.89(2) | 2.723(3) | 145(4) | |
| O8–H8···O2 | 1.05(6) | 1.65(6) | 2.699(3) | 171(5) | |
| O9–H9···O4 | 0.95(5) | 1.83(4) | 2.672(3) | 147(3) | |
| O10–H10···O3 | 0.97(2) | 1.74(3) | 2.670(3) | 160(3) | |

*Symmetry codes*: (i) $-x$, $1-y$, $1-z$; (ii) $1-x$, $1-y$, $-z$; (iii) $x$, $-1+y$, $z$; (iv) $-0.5+x$, $0.5-y$, $z$; (v) $0.5-x$, $-0.5+y$, $1-z$; (vi) $-x$, $-y$, $1-z$; (vii) $0.5-x$, $-0.5+y$, $-z$; (viii) $0.5-x$, $0.5+y$, $-z$; (ix) $0.5-x$, $0.5+y$, $1-z$; (x) $0.5+x$, $0.5-y$, $z$; (xi) $1-x$, $-y$, $-z$; (xii) $x$, $1+y$, $z$.

- Environment of Rb(2)/K(2): Three oxygen atoms belonging to $SO_4$ tetrahedron, one to $Te(1)O_6$ octahedron, three oxygen atoms to the same $Te(2)O_6$ and two to another $Te(2)O_6$ octahedron. The Rb(2)/K(2)–O distances vary from 2.857(2) to 3.241(2) Å.

We note that the values of Rb/K–O distances are close to those observed in $Rb_2SO_4Te(OH)_6$ material but slightly more longer than those found in $K_2SO_4Te(OH)_6$. Indeed, in $Rb_2SO_4 \cdot Te(OH)_6$ the Rb–O distances spread from 2.907(4) to 3.242(5) Å [6] whereas in $K_2SO_4Te(OH)_6$ structure, the K–O distances vary from 2.713 to 2.987 [2].

As mentioned before, both the sulfate and the tellurate groups, in the $Rb_{1.25}K_{0.75}SO_4Te(OH)_6$ structure, are connected with O–H···O hydrogen bonds. In fact, as in the original compound, $Rb_2SO \cdot Te(OH)_6$, six hydrogen bonds are detected. It should be noted that all hydrogen atoms belonging to $Te(OH)_6$ octahedra participate in the formation of hydrogen bonding. The O···H distances vary from 1.65(6) to 1.89(2) Å and the O–H···O angles have value between 145(4)° and 171(5)°. The hydrogen bonds

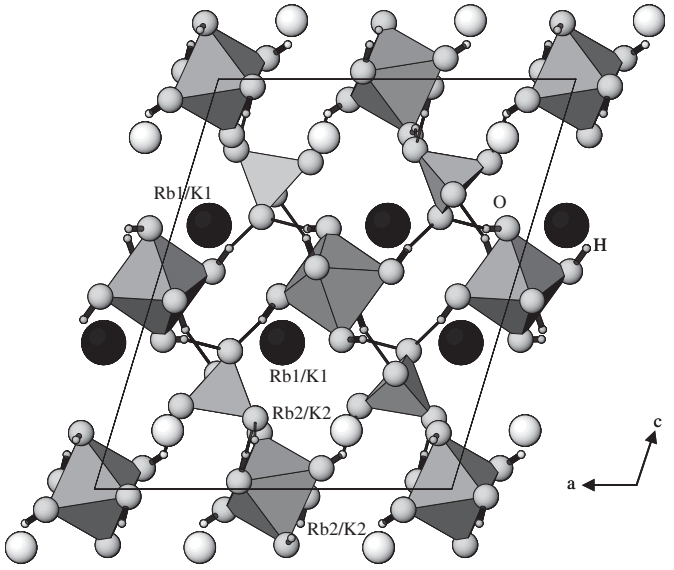


Fig. 2. Projection of $Rb_{1.25}K_{0.75}SO_4Te(OH)_6$ crystal structure on the *ac* plane.

are classical with O···O distances ranging from 2.670(3) to 2.778(3) Å with an average of 2.71 Å. In consequence, we can confirm, using NOVAK criterion [17], that there are two types of hydrogen bonds. In sulfate group, two oxygen atoms, O(3) and O(4), are tied to one hydrogen atom (Table 6), but each other oxygen atoms (O(1) and O(2)) are linked to two hydrogen atoms.

The presence of the O–H···O hydrogen bonds and all these values of O···H and O–H···O distances can favor the appearance of high conductivity at high temperature which is the cause of the superprotonic phase transition characterized by the bricking of hydrogen bonds which tie anionic groups. This fact leads us to complete the electrical studies.

### 3.2. Electrical properties

The most commonly used experimental technique to characterize the dynamics of diffusing ions in glasses and crystals is electrical relaxation measurements [20]. The measurements give us immediately the complex impedance, $Z^* = Z' - iZ''$ and complex conductivity $\sigma^* = \sigma + i\sigma''$, related to $Z^*$ by the relation: $\sigma^* = e/sz^*$, where $e$ and $s$ are the length and the area of the sample, respectively. The complex electric modulus $M^*$ is related to the impedance by the relation: $M^* = i\omega C_0 Z^*$, $C_0$ is the vacuum capacitance of the cell [21]. Thus, $Z^*$, $\sigma^*$ and $M^*$ are just alternative and interchangeable representations of the same macroscopic electric relaxation data.

The electrical conductivity and dielectric relaxation of $CsKSO_4Te(OH)_6$ have been studied [13]. We have shown in our previous work that the temperature variation of the DC conductivity, $\log(\sigma_0 T)$ versus $1000/T$ exhibits three regions:

- The first one, below 470 K. The conductivity in this region is about $5 \times 10^{-8}\,\Omega^{-1}\,cm^{-1}$ and the Arrhenius law: $\sigma T = \sigma_0 \exp(-E_a/kT)$ is not obeyed.
- The second region is between 470 and 590 K. In this region, the conductivity plot, exhibits two parts with transition at about 550 K attributed to the ferroelectric–paraelectric phase transition [10]. The Arrhenius law is obeyed on both sides of the temperature transition. The activation energies below and above this transition are, respectively, $E_{a1} = 1.29$ eV and $E_{a2} = 1.72$ eV. The difference can be attributed to the difficulty of the proton displacement caused by the cell deformation introduced with the establishment of the polar phase [22].
- The third region is above 590 K. The Arrhenius law is also obeyed in this region. An unusual high conductivity ($1 \times 10^{-4}\,\Omega^{-1}\,cm^{-1}$) and low activation energy ($E_{a3} = 0.30$ eV) are observed at 590 K. This behavior characterizes a superionic–protonic phase transition in $CsKSO_4Te(OH)_6$ [23].

The crystal with the conductivity, $\Omega \geqslant 10^{-4}\,\Omega^{-1}\,cm^{-1}$ is classified as a fast ionic conductor. Hence, $CsK(SO_4)\cdot Te(OH)_6$ material becomes a fast ionic conductor at high temperature ($T > 580$ K). We have also shown that the frequency dependence of AC ionic conductivity increases as a power of frequency. This behavior indicates that the frequency dependence of conductivity follows the Jonscher's law [24] as expected for most of the hopping type of the ionic conductors ($\sigma(\omega) = \sigma_0 + A\omega^n$ where $\sigma_0$ is the DC conductivity of the sample, $(0 < n < 1)$ is the power law exponent and $A$ is a constant for a particular temperature). The exponent $n$ shows temperature independent and remains almost constant about 0.55.

In order to examine the effect of the cationic substitution on the physical properties, we have extend our research to the rubidium potassium sulfate tellurate mixed solution $Rb_{1.25}K_{0.75}SO_4Te(OH)_6$. The complex impedance plane data ($-Z''$ versus the real part $Z'$) shows semicircle at high temperatures ($T > 480$ K). Thus, the pellet can be regarded as a parallel combination of resistance and capacitance in the electrical circuit. The DC resistance ($R$) at various temperatures is determined by extrapolation of the circular arc based on the Cole–Cole formulation. The DC conductivity ($\sigma_0$) is converted from the resistance by the relation $\sigma_0 = e/sR$, where $s$ and $e$ are the area and the thickness of the pellet, respectively. The temperature variation of the DC conductivity, $\log(\sigma_0 T)$ versus $1000/T$ is shown in Fig. 3. We note essentially the presence of two regions. The first one, below 450 K, characterizes the conductivity at low temperature. In this region, the conductivity is not linear so the Arrhenius law: $\sigma T = \sigma_0 \exp(-E_a/kT)$ is not obeyed. The second one between 460 and 570 K with a substantial jump characterizing the superionic–protonic phase transition in $Rb_{1.25}K_{0.75}SO_4Te(OH)_6$. Indeed, the conductivity jumps from $10^{-6}\,\Omega^{-1}\,cm^{-1}$ at 465 K to $10^{-4}\,\Omega^{-1}\,cm^{-1}$ at 570 K. The conductivity plot exhibits two parts with transition at about 510 K attributed to the ferroelectric–paraelectric

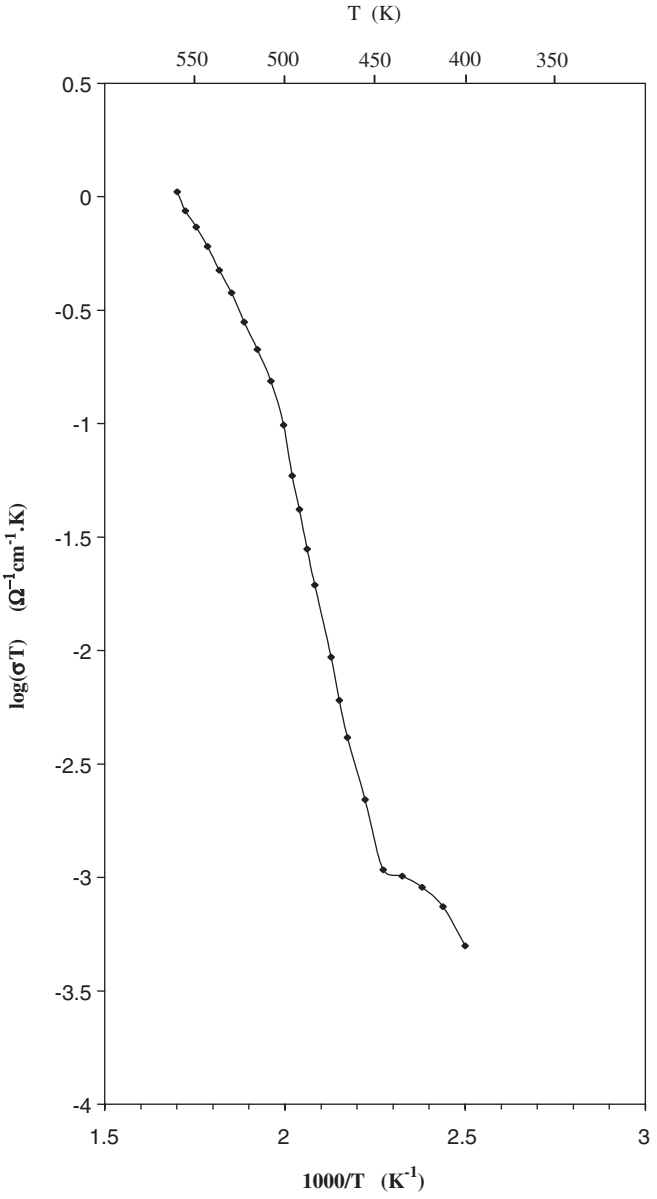


Fig. 3. Plot of DC conductivity $\log(\sigma_0 T)$ versus $1000/T$ for $Rb_{1.25}K_{0.75}SO_4Te(OH)_6$.

phase transition [10]. The Arrhenius law is obeyed on both sides of the temperature transition. The activation energies below and above this transition are, respectively, $E_{a1} = 1.35\,eV$ and $E_{a2} = 0.6\,eV$.

In most of ionic crystals, the contribution to the conductivity is determined by the concentrations of vacant sites as well as the ion mobility. Both of them are thermally activated and the activation energy contained the energy of defect formation and migration of charge carrier. The conduction in $Rb_{1.25}K_{0.75}SO_4Te(OH)_6$ is probably due to the hopping of protons among the dynamical disordered proton sites at high temperature. In fact, the increasing temperature induces the breaking of hydrogen bonds which link all the polyhedra. In consequence, the proton $H^+$ becomes free between the potential holes $TeO_6^{6-}$ and $SO_4^{2-}$.

For a close inspection of the relaxation dynamics, the dielectric relaxation is studied in the complex modulus formalism $M^*$. For a given temperature and a frequency, the real part $M'$ and the imaginary part $M''$ of the complex modulus have been also calculated from the complex impedance data by the relations $M' = \omega C_0 Z''$ and $M'' = \omega C_0 Z'$, $C_0$ is the vacuum capacitance of the cell and $\omega$ is the angular frequency of the electric field. This formalism has the advantage to eliminate the contribution of electrode polarization and other interfacial effects in solid electrolytes [22,25–27]. The frequency variation of the normalized imaginary part of the complex modulus ($M''/M''_{max}$) curves at various temperatures is shown in Fig. 4. Each isothermal frequency spectra exhibits a well defined peak. As one can see from Fig. 4, the peak positions of $M''/M''_{max}$ shift with temperatures. As temperature increases, the modulus peak maxima, ($\omega_m \tau = 1$, where $\tau$ is the most probable ion relaxation time), move toward higher frequency. The relaxation peaks cannot be observed at temperatures above 560 K due the uncovered high frequencies in this measurement. From Fig. 4, it can be seen that the $M''/M''_{max}$ curves are not symmetric, in concordance with the non-exponential behavior of the electrical function, that is well described

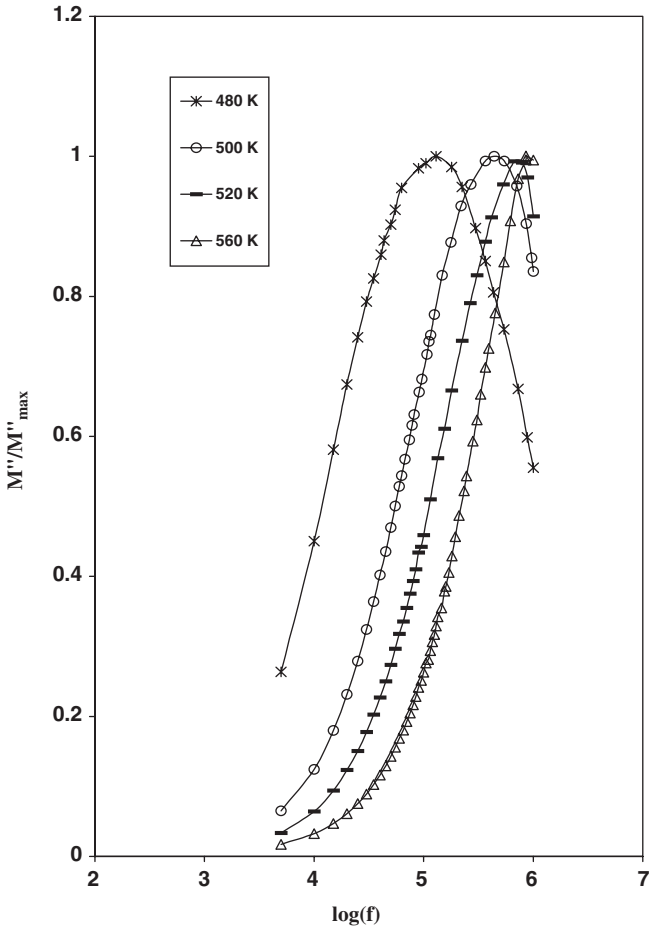


Fig. 4. Plot of the normalized imaginary part of modulus $M''/M''_{max}$ versus $\log(f)$ for $Rb_{1.25}K_{0.75}SO_4Te(OH)_6$ at various temperatures.

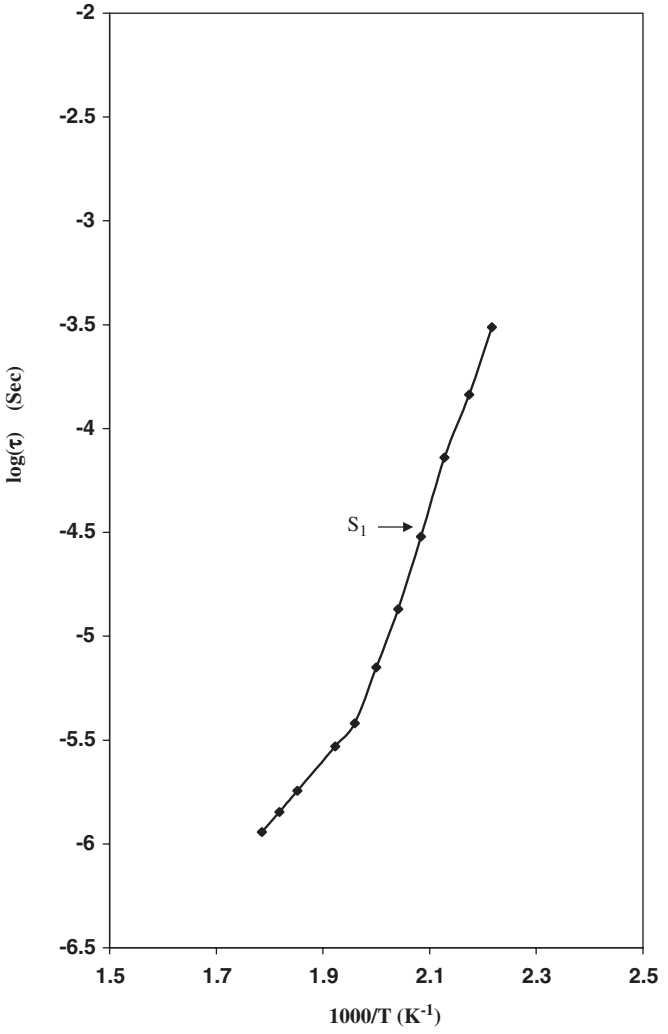


Fig. 5. Temperature dependence of relaxation time of $Rb_{1.25}K_{0.75}SO_4Te(OH)_6$.

by the empirical Kohlrausch function: $\varphi(t) = \exp[-(t/\tau)^{\beta}]$ $(0<\beta<1)$ [28,29].

The temperature dependence of the relaxation time is plotted in Fig. 5. The obtained curve also exhibits two parts with transition at about 515 K. It shows that the relaxation time appears thermally activated and can be described by Arrhenius law $\tau = \tau_0 \exp(E_m/(k_B T)$, where $\tau_0$ is the pre-exponential factor, $E_m$ is the activation energy from modulus, $k_B$ is Boltzmann's constant and $T$ is the absolute temperature. The activation energy $E_m$ obtained from the first and the second segment are 1.49 and 0.59 eV, respectively.

## 4. Conclusion

The structures of $CsK(SO_4)\cdot Te(OH)_6$ and $Rb_{1.25}K_{0.75}SO_4Te(OH)_6$ have been determined on single crystal. The structures appear to be similar for all the other sulfate tellurate compounds so far investigated. However, the examination of the local environments for all atoms reveals significant differences. The main interest of these structures is the presence of two different and independent anionic groups in the same unit cell connected by hydrogen bonds to form infinite rows parallel on the $(\bar{1}01)$ direction. The $CsK(SO_4)\cdot Te(OH)_6$ crystallizes in the monoclinic system with *Pn* space group. The two cesium cations in $CsKSO_4Te(OH)_6$ structure are coordinated by eight oxygen atoms (Cs(1)) and seven oxygen atoms (Cs(2)) whereas both K(1) and K(2) are surrounded by six oxygen atoms. The substitution of the cesium by the rubidium changes the space group from *Pn* to $P2_1/a$ and the two cations ($Rb^+$ and $K^+$) become statistically disordered on one atomic position. The Rb/K atoms in $Rb_{1.25}K_{0.75}SO_4Te(OH)_6$ are distributed on two sites and they are nine coordinated.

Electrical study shows that the presence of hydrogen bonds in $Rb_{1.25}K_{0.75}SO_4Te(OH)_6$ is the origin of superprotonic phase transition which appears in a strong jump in the conductivity plot. A relaxation study shows that the $H^+$ transfer is probably provided by a hoping mechanism. Other compounds with different substitution rate will be studied soon.

## References

[1] H. Khemakhem, Ferroelectrics 234 (1999) 47.
[2] R. Zilber, A. Durif, M.T. Averbuch-Pouchot, Acta Crystallogr. B 36 (1980) 2743.
[3] R. Zilber, A. Durif, M.T. Averbuch-Pouchot, Acta Crystallogr. B 37 (1981) 650.
[4] R. Zilber, A. Durif, M.T. Averbuch-Pouchot, Acta Crystallogr. B 38 (1982) 1554.
[5] M. Dammak, H. Khemakhem, T. Mhiri, A.W. Kolsi, A. Daoud, J. Solid State Chem. 145 (1999) 612.
[6] M. Dammak, H. Khemakhem, T. Mhiri, A.W. Kolsi, A. Daoud, J. Alloys Compds. 280 (1998) 107.
[7] M. Dammak, H. Khemakhem, T. Mhiri, J. Phys. Chem. Solids 62 (2001) 2069.
[8] M. Dammak, T. Mhiri, J. Jaud, J.M. Savariault, J. Inorg. Mater. 3 (2001) 861.
[9] H. Litaiem, M. Dammak, T. Mhiri, A. Coussou, J. Alloys Compds. 396 (2005) 34.
[10] N. Chabchoub, H. Khemakhem, M. Gargouri, J. Alloys Compds. 359 (2003) 84.
[11] C. Boudaya, N. Chabchoub, H. Khemakhem, R. Von der Mühll, J. Alloys Compds. 352 (2003) 304.
[12] N. Chabchoub, H. Khemakhem, R. Von der Mühll, J. Alloys Compds. 386 (2004) 319.
[13] N. Chabchoub, H. Khemakhem, J. Alloys Compds. 370 (2004) 8.
[14] A.J.M. Duisenberg, L.M.J. Kroon-Batenburg, A.M.M. Schreurs, J. Appl. Crystallogr. 36 (2003) 220.
[15] V. Petricek, M. Dusek, The Crystallographic Computing System Jana, Institute of Physics, Praha, Czech Republic, 2000.
[16] M. Dammak, L. Ktari, A. Cousson, T. Mhiri, J Solid State Chem. 178 (2005) 2109.
[17] A. Novak, Hydrogen Bonding in Solids, Springer, Berlin, Heidelberg, New York, 1974 (p. 177).
[18] L. Ktari, M. Dammak, T. Mhiri, J.-M. Savariault, J Solid State Chem. 161 (2001) 1.
[19] M. Abdelhedi, M. Dammak, A. Cousson, A.W. Kolsi, J. Alloys Compds. 398 (2005) 55.
[20] K.L. Ngai, R.W. Rendell, Phys. Rev. B 61 (2000) 14.
[21] P.B. Macedo, C.T. Mognihan, R. Bose, Phys. Chem. Glasses 13 (1972) 171.

[22] M. Dammak, H. Khemakhem, N. Zouari, A.W. Kolsi, T. Mhiri, Solid State Ionics 127 (2000) 125.
[23] H. Khemakhem, T. Mhiri, A. Daoud, Solid State Ionics 117 (1999) 337.
[24] A.K. Jonscher, J. Mater. Sci. 13 (1978) 553.
[25] D.P. Almond, A.R. West, R. West, R. Grant, Solid State Commun. 44 (1982) 1277.
[26] B.V.R. Chowdari, K. Radhakrishnan, J. Non-Cryst. Solids 101 (1989) 101.
[27] B.V.R. Chowdari, K. Radhakrishnan, J. Non-Cryst. Solids 108 (1989) 323.
[28] F.S. Howell, R.A. Bose, P.B. Macedo, C.T. Moynihan, J. Phys. Chem. 78 (1974) 639.
[29] K.L. Ngai, S.W. Martin, Phys. Rev. B 40 (1989) 10550.